Journal of Solid Mechanics Vol. 8, No. 1 (2016) pp. 58-77

Reflection and Transmission at the Boundary of Two Couple Stress Generalized Thermoelastic Solids

R. Kumar [1, *], K. Kumar [2], R.C. Nautiyal [2]

[1] *Department of Mathematics, Kurukshetra University, Kurukshetra, Haryana, 136119, India*
[2] *Department of Mathematics, DeenBandhu Chhotu Ram University of Science and Technology, Sonipat, Haryana, 131001, India*

Received 23 September 2015; accepted 10 December 2015

ABSTRACT

In this paper the reflection and transmission at a plane interface between two different couple stress generalized thermoelastic solid half spaces in context of Loard-Shulman(LS)[1967] and Green-Lindsay(GL)[1972] theories in welded contact has been investigated. Amplitude ratios of various reflected and transmitted waves are obtained due to incidence of a set of coupled longitudinal waves and coupled transverse waves. It is found that the amplitude ratios of various reflected and transmitted waves are functions of angle of incidence, frequency and are affected by the couple stress properties of the media. Some special cases are deduced from the present formulation.

Keywords : Couple stress thermoelastic solid; Longitudinal wave; Transverse wave; Reflection; Transmission; Amplitude ratios.

1 INTRODUCTION

VOIGT[1] was the first to introduce the concept of couple stress in the material, by assuming that, the interaction between two parts of the continuum not only depends on force stress vector but also on the couple stress vector. This leads to the description of stresses by means of the two skew symmetric tensors namely force stress tensor and couple stress tensor. However Cosserat and Cosserat [2] gave the mathematical formulation to analyze material with couple stresses, by considering that deformation of the medium is described by displacement vector and an independent rotation vector. Displacement and rotation are associated with skew symmetric stresses and couple stresses through constitutive relations. Later on many alternative theories were given on the same idea.

Toupin [3] studied the elastic materials with couple-stresses. Mindlin and Tiersten [4] investigated effects of couple-stresses in linear elasticity. Influence of the couple stresses concentration was given by Mindlin [5]. Koiter [6] studied couple stresses in the theory of elasticity. Experimental study of micropolar and couple stress elasticity in compact bone in bending was done by Yang and Lakes [7]. Yang et al. [8] have developed a couple stress theory, in which the strain energy has been shown to be quadratic function of the strain and symmetric curvatures and only a single material length scale parameter is involved. Sengupta and Ghosh [9] derived the frequency equation for couple stress elastic layer and deduced it for Rayleigh and Love wave propagation. Sengupta and Ghosh [10] investigated the problem of the propagation of waves in an elastic layer under the influence of couple stresses. Sengupta and Benerji [11] investigated the effects of couple stresses on the propagation of waves in elastic layer immersed in an infinite liquid. Georgiadis and Velgaki [12] studied the dispersive nature of Rayleigh waves propagation along the surface of a half-space at high frequencies using couple stress theory. Lubarda and Markenscoff [13] derived general conservation law for couple stress theory. Bardet and Vardoulakis [14] discussed

*Corresponding author.
E-mail address: Rajneesh_kuk@rediffmail.com (R. Kumar).

the importance of couple stresses in granular medium. Lubarda [15] applied the couple stress theory to the study of anti plane strain problem of circular inclusions. The problem of multiply-connected materials with holes and multi-phase simply connected materials have been addressed in the review article by Jasiuk and Strazenski [16]. Akgoz and Civalek [17] has analyzed the micro sized plates resting on elastic medium using modified couple stress theory . Recently, Sharma and Kumar [18] studied the velocity dispersion in an elastic plate with microstructure: effects of characteristic length in a couple stress model.

Biot [19] formulated the theory of coupled thermoelasticity to eliminated the paradox inherent in the classical uncoupled theory that elastic changes have no effect on the temperature. The heat equations for the both theories are of parabolic type predicting infinite speeds of propagation for heat waves contrary to physical observations. Lord and Shulman [20] introduced relaxation time to explain the propagation of a thermal wave and presented a modified theory called generalized theory of thermoleasticity (termed as LS theory). Using two relaxation time, Green and Lindsay [21] developed another generalized theory of thermoelasticity(termed as GL theory). Ram and Sharma [22] discussed reflection and transmission of micropolar thermoelastic waves with an imperfect bonding. Xue et al. [23] studied reflection and refraction of longitudinal displacement wave at interface between two micropolar elastic solid. Kumar et al. [24] presented reflection and transmission between two micropolar thermoelastic half-spaces with three-phase-lag model.

In the present paper, the reflection and refraction phenomenon at a plane interface between two couple stress generalized thermoelastic solid medium has been analyzed. In couple stress thermoelastic solid medium, potential functions are introduced to represent two longitudinal waves and two transverse waves. The amplitude ratios of various reflected and refracted waves to that of incident wave are derived numerically and depicted graphically.

2 BASIC EQUATIONS

Following Mindlin-Terstein [4], Loard-Shulman [20] and Green-Lindsay [21] the governing equations in couple-stress generalized thermoelastic solid are given by:

$$t_{ji,j} = \rho \ddot{u}_i \tag{1}$$

$$m_{ji,j} + e_{ijk} t_{jk} = 0 \tag{2}$$

$$K * \nabla^2 T - \rho c_e \left(\frac{\partial T}{\partial t} + \tau_0 \frac{\partial^2 T}{\partial t^2} \right) = T_o \beta \left(\frac{\partial u_{i,i}}{\partial t} + \tau_0 n_o \frac{\partial^2 u_{i,i}}{\partial t^2} \right) \tag{3}$$

$$t_{ij} = \lambda \varepsilon_{kk} \delta_{ij} + 2\mu \varepsilon_{ij} - \frac{1}{2} e_{ijk} m_{lk,l} - \beta \left(1 + \tau_1 \frac{\partial}{\partial t} \right) T \delta_{ij} \tag{4}$$

$$m_{ij} = 4\alpha k_{ji} + 4\beta' k_{ij} \tag{5}$$

$$k_{ij} = \phi_{j,i} \tag{6}$$

$$\phi_i = \frac{1}{2} e_{ipq} u_{q,p} \tag{7}$$

where t_{ij} is the stress components, ε_{ij} is the strain components, u_i is displacement components, m_{ij} is the couple-stress components, δ_{ij} is Kronecker's delta, e_{ijk} is alternate tensor, k_{ij} is curvature tensor, ρ is the density, ϕ_i is rotational vector, τ_0, τ_1 are thermal relaxation times with $\tau_1 \geq \tau_0 \geq 0$. Here $n_o = 1, \tau_1 = 0$, for L-S theory and $n_o = 0$ for G-L theory.

Eq.(1) with the help of Eqs. (2), (4)-(7) and without loss of generality assuming that $\beta' e_{lpq} e_{ijk} u_{q,pkl} = 0$ takes the form

$$\rho\ddot{u}_i = (\lambda+\mu)u_{j,ij} + \mu\nabla^2 u_i + \alpha\left(e_{ijk}e_{kpq}u_{q,pi}\right),_{ll} - \beta\left(1+\tau_1\frac{\partial}{\partial t}\right)T,_i \tag{8}$$

3 FORMULATION OF THE PROBLEM

We consider two couple stress homogenous isotropic generalized thermoelastic solid half spaces medium M_1 $\left(0<x_3<\infty\right)$ and medium $M_2\left(-\infty<x_3<0\right)$. The two media are in contact with each other at the plane $x_3=0$ of the rectangular Cartesian coordinate system (x_1,x_2,x_3) with an origin on the surface $x_3=0$ and x_3 axis pointing vertically downwards into the medium M_1. We choose x_1 axis in the direction of wave propagation so that all particle on the line parallel to x_2 axis are equally displaced. Therefore all the field quantities are independent of x_2. For two dimensional problems, we assume the displacement vector as:

$$u_i = (u_1, 0, u_3) \tag{9}$$

We introduce the potential functions ϕ and ψ through the relation:

$$u_1 = \frac{\partial\varphi}{\partial x_1} - \frac{\partial\psi}{\partial x_3}, u_3 = \frac{\partial\varphi}{\partial x_3} + \frac{\partial\psi}{\partial x_1} \tag{10}$$

We define the dimensionless quantities as:

$$\begin{aligned} &x_1' = \frac{\omega^*}{c_1}x_1, x_3' = \frac{\omega^*}{c_1}x_3, t' = \omega^* t, t_{ij}' = \frac{t_{ij}}{\beta T_0}, m_{ij}' = \frac{\omega^* m_{ij}}{c_1\beta T_0}, c_1^2 = \frac{\lambda+2\mu}{\rho}, \omega^{*2} = \frac{\lambda^2}{\mu^2 t^2+\rho\alpha}, \\ &u_1' = \frac{\omega^*}{c_1}u_1, u_3' = \frac{\omega^*}{c_1}u_3, T' = \frac{T}{T_0}, \tau_1' = \omega^*\tau_1, \tau_0' = \omega^*\tau_0, t_0' = \omega^* t_0, h' = \frac{c_1 h}{\omega^*} \end{aligned} \tag{11}$$

Upon introducing the quantities defined by Eq. (11) in Eq. (8) and with the aid of (4)-(7), (9) and (10) after suppressing the primes, we obtain

$$\nabla^2\phi - a_{13}\left(1+\tau_1\frac{\partial}{\partial t}\right)T = \ddot{\phi} \tag{12}$$

$$\nabla^2\psi - a_{12}\nabla^4\psi = \frac{c_1^2}{c_2^2}\ddot{\psi} \tag{13}$$

$$\nabla^2 T - a_6\left(\frac{\partial T}{\partial t} + \tau_0\frac{\partial^2 T}{\partial t^2}\right) = a_7\delta_{ij}\left(\frac{\partial u_{i,j}}{\partial t} + \tau_0 n_o\frac{\partial^2 u_{i,j}}{\partial t^2}\right) \tag{14}$$

$$t_{ij} = a_1\delta_{ij}e + a_2\left(u_{i,j} + u_{j,i}\right) - a_3 e_{ijk}e_{kpq}u_{q,pll} - \beta\left(1+\tau_1\frac{\partial}{\partial t}\right)T\,\delta_{ij} \tag{15}$$

$$m_{ij} = a_4 e_{ipq}u_{q,pj} + a_5 e_{jpq}u_{q,pi} \tag{16}$$

where

$$a_1=\frac{\lambda}{\beta T_0},a_2=\frac{\mu}{\beta T_0},a_3=\frac{\alpha\omega^{*2}}{c_1^2\beta T_0},a_4=\frac{2\alpha\omega^{*2}}{c_1^2\beta T_0},a_5=\frac{2\beta'\omega^{*2}}{c_1^2\beta T_0},b_1=\frac{\rho c_e c_1^2}{K^*\omega^*},b_2=\frac{c_1^2\beta}{K^*\omega^*},$$
$$a_8=\frac{\mu}{\lambda+\mu},a_9=\frac{\alpha\omega^{*2}}{c_1^2(\lambda+\mu)},a_{10}=\frac{\beta T_0}{\lambda+\mu},a_{11}=\frac{\rho c_1^2}{\lambda+\mu},a_{12}=\frac{a_9}{a_8},a_{13}=\frac{a_{10}}{1+a_8}$$

The Eq. (13) corresponds to purely transverse wave mode that decouples from rest of the motion and is not affected by the thermal effect but affected by the effect of couple stress.We assume the solution of the form

$$(\phi,\psi,T)=(\phi_1,\psi_1,T_1)e^{\{i(k(x_1\sin\theta-x_3\cos\theta)-\omega t)\}} \tag{17}$$

where k is the wave number and ω is the circular frequency.Substituting the values of ϕ,ψ and T from Eq.(17) in Eqs. (12)-(14), we obtain

$$AV^4+BV^2+C=0 \tag{18}$$

$$DV^4+EV^2+F=0 \tag{19}$$

where $V=\frac{\omega}{k}$ is the velocity of waves, and $A=l_1a_7,B=-a_7l_1-1-i\,\omega a_5a_8l_2l_3,C=1,D=\frac{c_1^2}{a_6c_2^2},E=-\frac{1}{a_6},F=-\omega^2$.

Let the roots of the Eq. (18) be denoted by $V_i^2(i=1,2)$. Two positive values of V in the descending order will be the velocities of longitudinal waves(P) and thermal waves(T). Similarly, the roots of Eq. (19) be denoted by $V_i^2(i=3,4)$ and two positive roots of V of Eq. (19) are the velocities of reflected transverse waves (SV1 and SV2).

4 REFLECTION AND TRANSMISSION

We consider a longitudinal waves (P) or thermal waves (T) or transverse waves (SV1 or SV2) propagating through the medium M_1 and is incident at the plane $x_3=0$. Corresponding to each incident wave, we get reflected longitudinal wave (P), thermal wave (T), transverse waves (SV1 and SV2) in medium M_1 and transmitted longitudinal wave(P), thermal wave (T), transverse waves (SV1 and SV2) in medium M_2 as shown in Fig.1.

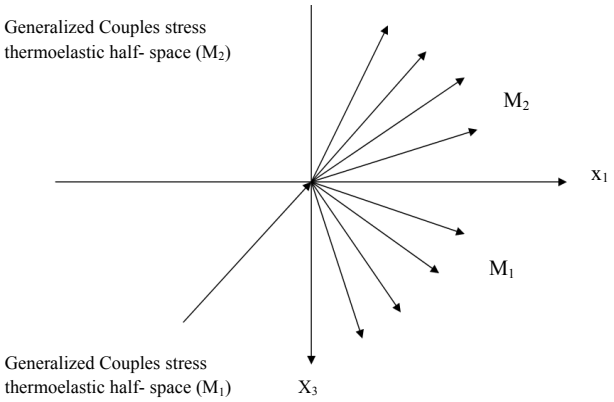

Fig.1
Geometry of the problem.

5 BOUNDARY CONDITIONS

5.1 Mechanical conditions

The boundary conditions are the continuity of normal stress, tangential stress, tangential couple stress, displacement components and rotations vector at the interface of two couple stress generalized thermoelastic solid half-spaces. Mathematically, these can be written as:

$$\left.\begin{array}{l} t_{33} = \bar{t}_{33} \\ t_{31} = \bar{t}_{31} \\ m_{32} = \bar{m}_{32} \\ u_1 = \bar{u}_1 \\ u_3 = \bar{u}_3 \\ \varphi_2 = \bar{\varphi}_2 \end{array}\right\} \quad at \quad x_3 = 0 \tag{20}$$

5.2 Thermal Condition

The thermal condition corresponding to insulated boundary is given by

$$\left.\begin{array}{l} T = \bar{T} \\ K * \dfrac{\partial T}{\partial x_3} = \bar{K} * \dfrac{\partial \bar{T}}{\partial x_3} \end{array}\right\} \quad at \quad x_3 = 0 \tag{21}$$

In view of (17) we assume the values of ϕ, ψ and T for medium M_1 as:

$$(\phi, T) = \sum_{i=1}^{2} (1, b_i) \left[A_{0i} e^{\{i(k(x_1 \sin\theta_{0i} - x_3 \cos\theta_{0i}) - \omega t)\}} + P_i \right] \tag{22}$$

$$\psi = \sum_{j=3}^{4} B_{0j} \left[e^{\{i(k(x_1 \sin\theta_{0j} - x_3 \cos\theta_{0j}) - \omega t)\}} + P_j \right] \tag{23}$$

We attach bar notation for medium M_2, then the values of $\bar{\phi}, \bar{\psi}$ and $\bar{T}$ are taken as:

$$(\bar{\phi}, \bar{T}) = \sum_{i=1}^{2} (1, \bar{b}_i) \left[\bar{A}_i e^{\{i(k(x_1 \sin\bar{\theta}_i + x_3 \cos\bar{\theta}_i) - \omega t)\}} \right] \tag{24}$$

$$\bar{\psi} = \sum_{j=3}^{4} \left[\bar{B}_j e^{\{i(k(x_1 \sin\bar{\theta}_j + x_3 \cos\bar{\theta}_j) - \omega t)\}} \right] \tag{25}$$

where

$$P_i = A_i e^{\{i(k(x_1 \sin\theta_i + x_3 \cos\theta_i) - \omega t)\}}, P_j = e^{\{i(k(x_1 \sin\theta_j + x_3 \cos\theta_j) - \omega t)\}}, b_i = \frac{(-1 + V_i^2) k^2}{a_5 (1 - ik V_i^2 \tau_1)}, \bar{b}_i = \frac{(-1 + \bar{V}_i^2) k^2}{\bar{a}_5 (1 - ik \bar{V}_i^2 \bar{\tau}_1)}$$

A_{0i} and $A_i\,(i = 1,2)$ are the amplitudes of incident and reflected longitudinal waves(P) and thermal waves (T) respectively, where B_{0j} and $B_j\,(j = 3,4)$ are the amplitudes of incident and reflected transverse waves (SV1 and

SV2) respectively. $\bar{A}_i\,(i=1,2)$ and $\bar{B}_j\,(j=3,4)$ are the amplitudes of transmitted plane waves(P), thermal waves (T) transmitted transverse waves (SV1 and SV2) respectively.

In order to satisfy the boundary conditions, the extension of Snell's law is given by

$$\frac{\sin\theta_0}{V_0}=\frac{\sin\theta_1}{V_1}=\frac{\sin\theta_2}{V_2}=\frac{\sin\theta_3}{V_3}=\frac{\sin\theta_4}{V_4}=\frac{\sin\bar{\theta}_1}{\bar{V}_1}=\frac{\sin\bar{\theta}_2}{\bar{V}_2}=\frac{\sin\bar{\theta}_3}{\bar{V}_3}=\frac{\sin\bar{\theta}_4}{\bar{V}_4} \tag{26}$$

where

$$V_1=V_2=V_3=V_4=\bar{V}_1=\bar{V}_2=\bar{V}_3=\bar{V}_4=V \quad at \quad x_3=0 \tag{27}$$

Making use of potentials given by Eqs. (22)-(25) in the boundary conditions given by Eqs. (20) and (21) and with aid of (26) and (27), we obtain a system of eight non-homogeneous equations, which can be written as:

$$\sum_{i,j=1}^{8} d_{ij} Z_j = Y_i \tag{28}$$

where

$$d_{1i}=-k^2a_9-k^2a_{10}\frac{1}{V_0^2}\left[\left(\frac{V_0}{V_i}\right)^2-\sin^2\theta_0\right]-\delta_1 b_i \quad , \quad d_{1j}=-k^2a_{10}\frac{1}{V_0^2}\left[\left(\frac{V_0}{V_j}\right)^2-\sin^2\theta_0\right]^{\frac{1}{2}}\sin\theta_j \quad ,$$

$$d_{1l}=k^2\bar{a}_9+k^2\bar{a}_{10}\frac{1}{V_0^2}\left[\left(\frac{V_0}{\bar{V}_i}\right)^2-\sin^2\theta_0\right]+\delta_1\bar{b}_i \quad , \quad d_{1m}=k^2\bar{a}_{10}\frac{1}{V_0^2}\left[\left(\frac{V_0}{\bar{V}_j}\right)^2-\sin^2\theta_0\right]^{\frac{1}{2}}\sin\bar{\theta}_j \quad ,$$

$$d_{2i}=-2a_{10}k^2\frac{1}{V_0^2}\left[\left(\frac{V_0}{V_i}\right)^2-\sin^2\theta_0\right]^{\frac{1}{2}}\sin\theta_i \quad , \quad d_{2j}=a_{10}k^2\frac{1}{V_0^2}\left[\left(\frac{V_0}{V_j}\right)^2-\sin^2\theta_0\right]+a_{11}k^4 \quad ,$$

$$d_{2l}=2\bar{a}_{10}k^2\frac{1}{V_0^2}\left[\left(\frac{V_0}{\bar{V}_i}\right)^2-\sin^2\theta_0\right]^{\frac{1}{2}}\sin\bar{\theta}_i \quad , \quad d_{2m}=-\bar{a}_{10}k^2\frac{1}{V_0^2}\left[\left(\frac{V_0}{\bar{V}_j}\right)^2-\sin^2\theta_0\right]^{\frac{1}{2}}+a_{11}k^4 \quad ,$$

$$d_{3j}=-a_{12}\frac{1}{V_0^2}\left[\left(\frac{V_0}{V_j}\right)^2-\sin^2\theta_0\right]^{\frac{1}{2}} \quad , \quad d_{3m}=\bar{a}_{12}\frac{1}{V_0^2}\left[\left(\frac{V_0}{\bar{V}_j}\right)^2-\sin^2\theta_0\right]^{\frac{1}{2}} \quad ,$$

$$d_{4i}=\sin\theta_i, d_{4j}=-a_{12}\frac{1}{V_0^2}\left[\left(\frac{V_0}{V_j}\right)^2-\sin^2\theta_0\right]^{\frac{1}{2}} \quad , \quad d_{4l}=-\sin\bar{\theta}_i, d_{4m}=\bar{a}_{12}\frac{1}{V_0^2}\left[\left(\frac{V_0}{\bar{V}_j}\right)^2-\sin^2\theta_0\right]^{\frac{1}{2}} \quad ,$$

$$d_{5i}=\frac{1}{V_0^2}\left[\left(\frac{V_0}{V_i}\right)^2-\sin^2\theta_0\right]^{\frac{1}{2}} \quad , \quad d_{5j}=\sin\theta_j, d_{5l}=-\frac{1}{V_0^2}\left[\left(\frac{V_0}{\bar{V}_i}\right)^2-\sin^2\theta_0\right]^{\frac{1}{2}}, d_{5j}=-\sin\bar{\theta}_j \quad ,$$

$$d_{6j}=-k^2 \quad , \quad d_{6l}=k^2d_{7i}=b_i \quad , \quad d_{7l}=-\bar{b}_i \quad , \quad d_{8i}=K^*b_i\frac{1}{V_0^2}\left[\left(\frac{V_0}{V_i}\right)^2-\sin^2\theta_0\right]^{\frac{1}{2}} \quad ,$$

$$d_{8l}=\bar{K}^*\bar{b}_i\frac{1}{V_0^2}\left[\left(\frac{V_0}{\bar{V}_i}\right)^2-\sin^2\theta_0\right]^{\frac{1}{2}} \quad , \quad i=1,2,\ j=3,4,\quad l=5,6,\quad m=7,8$$

$$Z_1=\frac{A_1}{A^*},Z_2=\frac{A_2}{A^*},Z_3=\frac{B_1}{A^*},Z_4=\frac{B_2}{A^*},Z_5=\frac{\bar{A}_1}{A^*},Z_6=\frac{\bar{A}_2}{A^*},Z_7=\frac{\bar{B}_1}{A^*},Z_8=\frac{\bar{B}_2}{A^*}$$

And

$$V_0=\{V_1 \quad \text{for incident } P-\text{Wave}$$
$$V_2 \quad \text{for incident } T-\text{Wave}$$
$$V_3 \quad \text{for incident } SV\,1-\text{wave}$$
$$V_4 \quad \text{for incident } SV\,2-\text{Wave}.\}$$

For incident P-wave:

$$A^*=A_{01}\ ,\ A_{02}=B_{01}=B_{02}=0\ ,$$
$$Y_1=-d_{11}\ ,\ Y_2=d_{21}\ ,\ Y_3=d_{31}\ ,\ Y_4=-d_{41}\ ,\ Y_5=d_{51}\ ,\ Y_6=d_{61}\ ,\ Y_7=-d_{71}\ ,\ Y_8=d_{81}$$

For incident T-wave:

$$A^*=A_{02}\ ,\ A_{01}=B_{01}=B_{02}=0\ ,$$
$$Y_1=-d_{12}\ ,\ Y_2=d_{22}\ ,\ Y_3=d_{32}\ ,\ Y_4=-d_{42}\ ,\ Y_5=d_{52}\ ,\ Y_6=d_{62}\ ,\ Y_7=-d_{72}\ ,\ Y_8=d_{82}$$

For incident SV1- wave:

$$A^*=B_{01}\ ,\ A_{01}=A_{02}=B_{02}=0\ ,$$
$$Y_1=d_{13}\ ,\ Y_2=-d_{23}\ ,\ Y_3=d_{33}\ ,\ Y_4=d_{43}\ ,Y_5=-d_{53}\ ,\ Y_6=-d_{63}\ ,\ Y_7=d_{73}\ ,\ Y_8=d_{83}$$

For incident SV2- wave:

$$A^*=B_{02}\ ,\ A_{01}=A_{02}=B_{01}=0\ ,$$
$$Y_1=d_{14}\ ,\ Y_2=-d_{24}\ ,\ Y_3=d_{34}\ ,\ Y_4=d_{44}\ ,Y_5=-d_{54}\ ,\ Y_6=-d_{64}\ ,\ Y_7=d_{74}\ ,\ Y_8=d_{84}$$

6 SPECIAL CASES

If $n_0=0,\tau_1>0$ in Eq. (28), gives the resulting expression for couple stress themoelastic medium with two relaxation times.

If $n_0=1,\tau_1=0$ in Eq. (28), gives the value of resulting expression for couple stress thermoelastic medium with one relaxation time.

If $\tau_0=\tau_1=0=n_0$ in Eq. (28), we find the resulting expression for couple stress thermoelastic media.

7 NUMERICAL RESULTS AND DISCUSSION

We now consider a numerical example to explain the analytical procedure presented earlier for LS and GL theories with couple stress effect and without couple stress effect. The absolute values of amplitude ratio are computed for the angle of incidence lying between $0^o\le\theta_0\le 90^o$. Numerical computations of these amplitude ratios are also made for the particular cases. The physical constants for medium M_1 are taken as:

$\bar{\lambda} = 2.238N\ /\ m^2, \bar{\mu} = 3.68N\ /\ m^2, \bar{\rho} = 8.965kg\ /\ m^3, \bar{c}_e = 1.04\times10^3 Jkg^{-1}\deg^{-1},$
$\bar{K}^* = 2.4\times10^2 Wm^{-1}\deg^{-1}, \bar{T}_0 = 298^o K, \bar{\alpha} = 1.5N, \bar{\beta} = 2.03Nm^{-1}\deg^{-1}, \beta_1' = 2.4N, \tau_0 = .613, \tau_1 = .513$

The physical constants for medium M_2 are as:

$\bar{\lambda} = 7.76N\ /\ m^2, \bar{\mu} = 3.28N\ /\ m^2, \bar{\rho} = 1.74kg\ /\ m^3, \bar{c}_e = 1.021\times10^3 Jkg^{-1}\deg^{-1},$
$\bar{K}^* = 1.7\times10^2 Wm^{-1}\deg^{-1}, \bar{T}_0 = 296^o K, \bar{\alpha} = 2.05N, \bar{\beta} = 2.68Nm^{-1}\deg^{-1}, \beta_1' = 1.5N, \tau_0 = .613, \tau_1 = .413.$

We have used MATLAB 7.12.0.635(R2011a) to find amplitude ratios for angle of incidence of the incident longitudinal wave(P), thermal wave(T) and incident transverse (SV-I and SV-II) waves. The amplitude ratios for reflected longitudinal waves reflected thermal waves reflected transverse waves in medium M_1 and corresponding transmitted waves in medium M_2 are shown graphically in Figs. 2-33.

In all the Figures  and  present the values of amplitude ratio for couple stress generalized thermoelastic solids in context of Lord-Shulman and Green-Lindsay theories and denoted by CLS and CGL respectively while the words WCLS and WCGL corresponds to the thermoelastic theory in context of Lord-Shulman and Green-Lindsay represented by  and  respectively. The variations of the amplitude ratios $|Z_i|, (i = 1,2,.....8)$ of various reflected and transmitted waves for CLS, CGL, WCLS and WCGL with angle of emergence θ_0 of different cases of the incident wave (P-, T-, SV1- or SV2-) have been shown in Figs. 2-33.

7.1 Incident P- wave

The variations of the absolute values of the amplitude ratios of various reflected and transmitted waves with angle of incidence varying from $0^o \le \theta_0 \le 90^o$ of incident P-wave have been shown in Figs. 2-9.

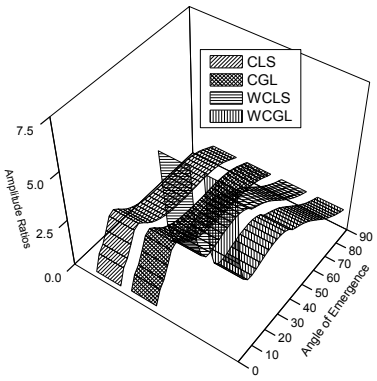

Fig.2
Variation of amplitude ratios of reflected P-waves versus angle of incidence.

Fig. 2 shows the variation of amplitude ratios of reflected P-wave with angle of emergence for CLS, CGL, WCLS and WCGL. It is seen that the values of amplitude ratios decrease for CLS and CGL for small values of angle of emergence and oscillate with increase in angle of emergence. The values of amplitude ratio for WCLS and WCGL theories increase for $0^o \le \theta_0 \le 20^o$. Also it is noticed the values of for WCLS is the largest for the small values of angle of emergence ($0^o \le \theta_0 \le 12^o$). For the intermediate values of angle of emergence the values of amplitude ratio for GL theory are the highest. The values of amplitude ratio for CLS are greater than the CGL, WCLS and WCGL as θ_0 increases.

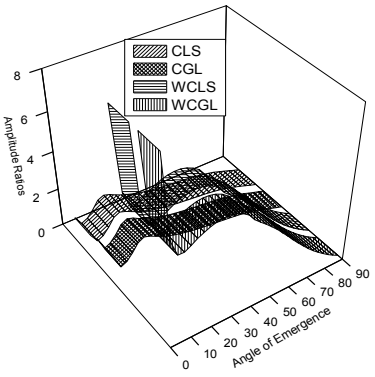

Fig.3
Variation of amplitude ratios of reflected T-waves versus angle of incidence.

Fig. 3 presents the variation of amplitude ratios of the reflected T-wave with angle of emergence θ_0 for various theories. It is noticed that values of amplitude ratio $|Z_2|$ decrease for all CLS, CGL, WCLS and WCGL for $0^o \le \theta_0 \le 10^o$ whereas the values of amplitude ratios oscillates for all the theories for intermediate values of angle of emergence and decrease smoothly as θ_0 increases for WCLS and WCGL.

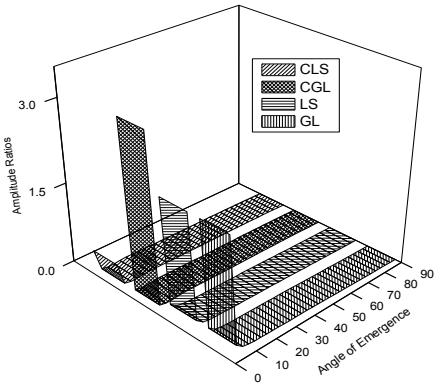

Fig.4
Variation of amplitude ratios of reflected SV1-waves versus angle of incidence.

The variations of amplitude ratios of reflected SV1- wave with angle of emergence for various theories are shown in Fig. 4. The values of amplitude ratio $|Z_3|$ decrease sharply for small values of angle emergence then decrease smoothly as the value of angle of emergence increases. The values of amplitude ratio $|Z_3|$ for CGL theory are greater for all values of angle of emergence.

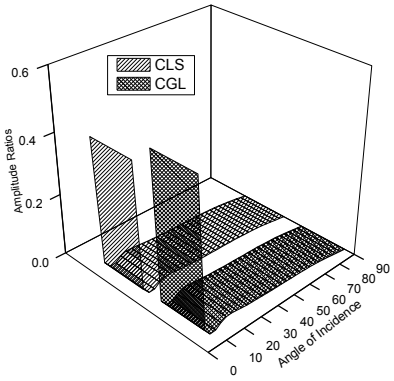

Fig.5
Variation of amplitude ratios of reflected SV2 -waves versus angle of incidence.

Fig. 5 depicts that variation of amplitude ratios of transmitted SV2- wave with angle of emergence. It is evident that values of amplitude ratio $|Z_4|$ decrease sharply for the initial value of angle of emergence and decrease smoothly for the large values of angle of emergence.

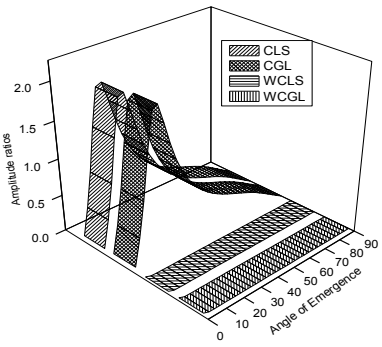

Fig.6
Variation of amplitude ratios of transmitted P-waves versus angle of incidence.

The variation of amplitude ratios $|Z_5|$ (transmitted P-wave) for different theories CLS, CGL, WCLS and WCGL are shown in Fig. 6. It can be seen that the values of $|Z_5|$ increase sharply for CLS and CGL theories for small values of angle of emergence then decrease smoothly whereas the values of amplitude ratios of transmitted P-wave for WCLS and WC have very low values in comparison to CLS and CGL.

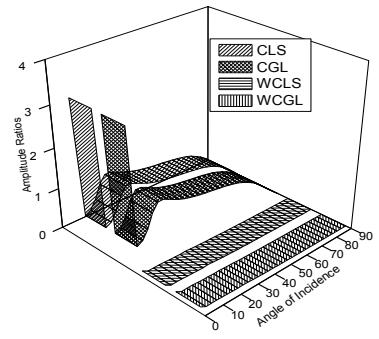

Fig.7
Variation of amplitude ratios of transmitted T -waves versus angle of incidence.

Fig. 7 shows the variation of amplitude ratios $|Z_6|$ of transmitted T-wave for CLS, CGL, WCLS and WCGL with respect to angle of emergence. The values of $|Z_6|$ decrease sharply for small values, oscillates for intermediate values and decrease for large values of angle of emergence for CLS and CGL.

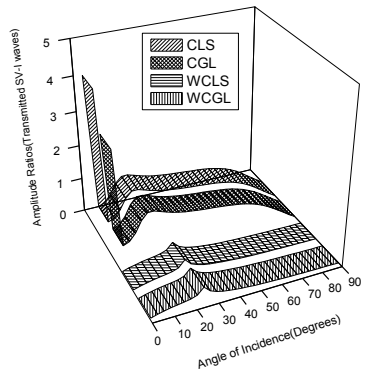

Fig.8
Variation of amplitude ratios of transmitted SV1-waves versus angle of incidence.

Fig. 8 represents the variation of amplitude ratios $|Z_7|$ of transmitted SV1- wave with respect to angle of emergence. It is noticed that the values of $|Z_7|$ decrease for $0^o \le \theta_0 \le 10^o$ for CLS and CGL and the values of amplitude ratio $|Z_7|$ for CLS are greater than CGL. The values of amplitude ratio $|Z_7|$ decrease for WCLS and WCGL for $0^o \le \theta_0 \le 33^o$, $45^o \le \theta_0 \le 90^o$ and behavior is reverse for the remaining values of angle of emergence for WCLS and WCGL.

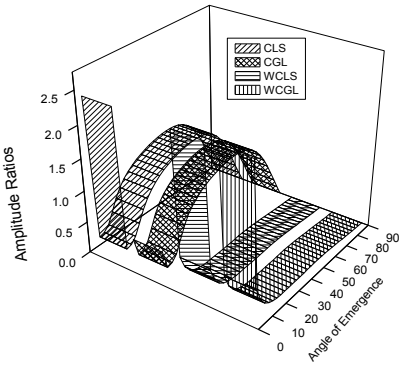

Fig.9
Variation of amplitude ratios of transmitted SV2 -waves versus angle of incidence.

Fig. 9 shows the variation of amplitude ratios $|Z_8|$ with respect to angle of emergence for CLS, CGL, WCLS and WCGL. It is observed that the values of $|Z_8|$ decrease sharply for small values of angle of emergence for all CLS, CGL, WCLS and WCGL. The values of $|Z_8|$ increase for $6^o \le \theta_0 \le 51^0$ for CLS theory and for $6^o \le \theta_0 \le 54^0$ for CGL and decrease for the remaining values of angle of emergence. The values of $|Z_8|$ oscillate for WCLS and WCGL.

7.2 Incident T-wave

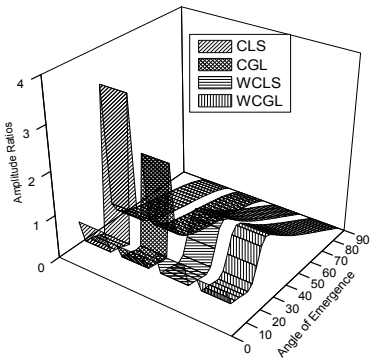

Fig.10
Variation of amplitude ratios of reflected P-waves versus angle of incidence.

It is clear from Fig. 10 that values of amplitude ratio $|Z_1|$ decrease for CLS, CGL, WCLS and WCGL with increase in angle of emergence (θ_0) from 0^o to 10^o then fluctuate in the range $10^o \le \theta_0 \le 50^o$ and decrease as θ_0 increase.

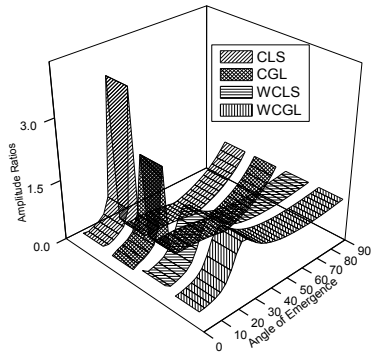

Fig.11
Variation of amplitude ratios of reflected T-waves versus angle of incidence.

Fig. 11 indicates that the values of amplitude ratio $|Z_2|$ increase in the range $0^o \le \theta_0 \le 20^o$ and fluctuate with the increase in the angle of emergence for CLS and CGL. But the values of $|Z_2|$ in case of CLS are higher in comparison to CGL.

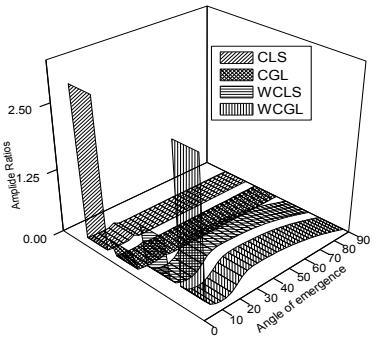

Fig.12
Variation of amplitude ratios of reflected SV1-waves versus angle of incidence.

Fig. 12 depicts the variation of amplitude ratio for reflected SV1- wave for CLS, CGL, WCLS and WCGL. It shows that the values of amplitude ratio $|Z_3|$ decrease sharply in the range $0^o \le \theta_0 \le 5^o$ for CLS and LS whereas the values of amplitude ratio $|Z_3|$ decrease smoothly for CGL and WCLS for small value of θ_0. The values of $|Z_3|$ oscillates for intermediate value of angle of emergence for all the cases and decrease smoothly as the angle of emergence (θ_0) increases.

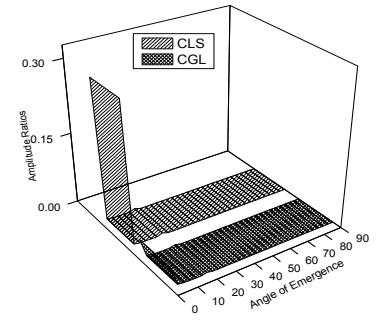

Fig.13
Variation of amplitude ratios of reflected SV2-waves versus angle of incidence.

Fig. 13 shows the variation of amplitude ratio $|Z_4|$ for reflected SV2- wave. The behavior of amplitude ratio for both CGL and CLS is similar with difference in magnitude value.

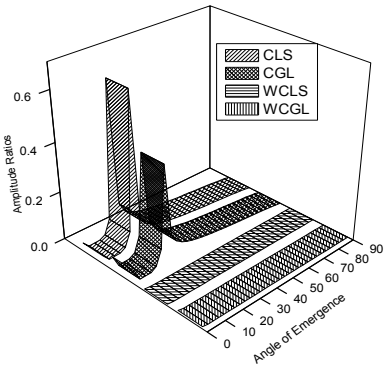

Fig.14
Variation of amplitude ratios of transmitted P-waves versus angle of incidence.

Fig. 14 shows the variation of amplitude ratio $|Z_5|$ for transmitted P-wave. The value of amplitude ratio decrease $|Z_5|$ in the range $0^o \le \theta_0 \le 3.5^o$ thereafter increase in the range $3.5^o \le \theta_0 \le 20^o$ and decrease as the angle of emergence increase for both CLS and CGL. The Values of amplitude ratio $|Z_5|$ fluctuate for WCLS and WCGL with the increase in angle of emergence. The values of amplitude ratio for WCLS and WCGL are very low in comparison to CLS and CGL.

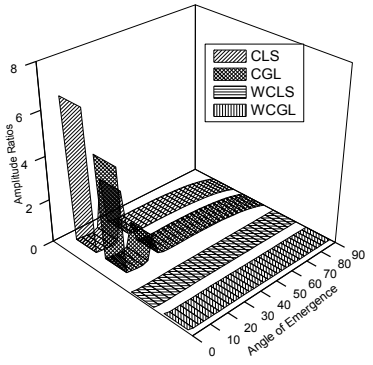

Fig.15
Variation of amplitude ratios of transmitted T-waves versus angle of incidence.

Fig. 15 shows the variation of amplitude ratio of $|Z_6|$ for transmitted T-wave. The values of amplitude ratio $|Z_6|$ decrease in the range $0^o \le \theta_0 \le 4.5^o$ thereafter increase in the range $4.5^o \le \theta_0 \le 15.5^o$ and decrease smoothly as the value of angle of emergence increase for CLS and CGL. Whereas the values of amplitude ratio $|Z_6|$ oscillate for WCLS and WCGL for all value of θ_0 .

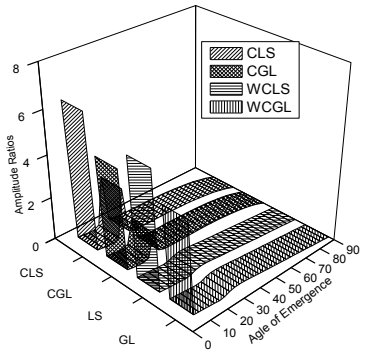

Fig.16
Variation of amplitude ratios of transmitted SV1-waves versus angle of incidence.

Fig. 16 represents the variation of amplitude ratio $|Z_7|$ for SV1- transmitted wave. It can be seen that values of amplitude ratio $|Z_7|$ behave alike for all CLS, CGL, WCGL and WCLS with difference in the magnitude values. The values of amplitude ratio decrease sharply for small values of θ_0 then oscillate for intermediate values and decrease as the angle of emergence increases.

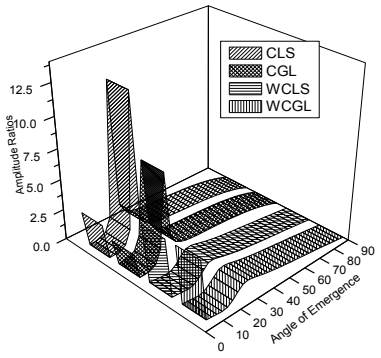

Fig.17
Variation of amplitude ratios of transmitted SV2-waves versus angle of incidence.

Fig. 17 depicts the variation of amplitude ratio $|Z_8|$ for transmitted SV2- wave. It can be observed that the values of amplitude ratio $|Z_8|$ decrease in the range $0^o \le \theta_0 \le 2.9^o$ for all the theories CLS CGL, WCLS and WCGL. The values of amplitude ratio $|Z_8|$ increase in the range $2.9^o \le \theta_0 \le 25^o$ and decrease smoothly as the angle of emergence increases for CLS and CGL theories. The values of amplitude ratio $|Z_8|$ increase in the range $2.9^o \le \theta_0 \le 31^o$ and decrease as the angle of emergence θ_0 increase for WCLS and WCGL.

7.3 Incident SV-1 wave

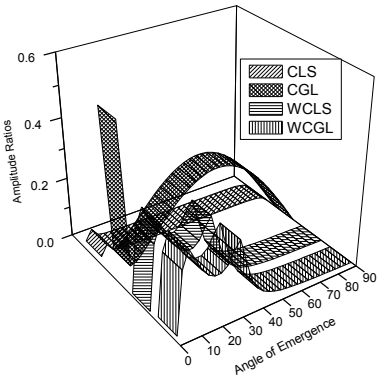

Fig.18
Variation of amplitude ratios of reflected P-waves versus angle of incidence.

Fig. 18 shows the variation of amplitude ratio $|Z_1|$ for reflected P-wave. The value of amplitude ratio $|Z_1|$ decrease sharply in the range $0^o \le \theta_0 \le 2.9^o$ thereafter increase in the range $2.9^o \le \theta_0 \le 50^o$ and decrease for the remaining value of angle of emergence for CGL. The value of amplitude ratio $|Z_1|$ increase in the range $0^o \le \theta_0 \le 2.5^o$ and decrease smoothly as the values of angle of emergence θ_0 increases for CLS. The values of amplitude ratio $|Z_1|$ increase in $0^o \le \theta_0 \le 3^o$, oscillate when $3^o \le \theta_0 \le 35^o$ and decrease for the remaining values of θ_0 for WCLS and WCGL.

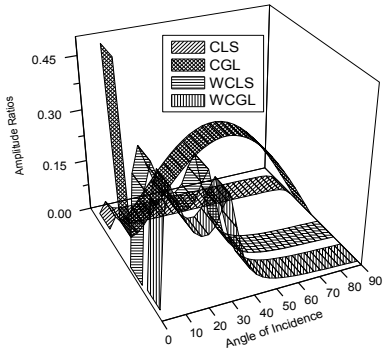

Fig.19
Variation of amplitude ratios of reflected T-waves versus angle of incidence.

Fig. 19 shows the variation of amplitude ratio $|Z_2|$ for reflected P-wave. It can be seen that the behavior of $|Z_2|$ and $|Z_1|$ is approximate similar with difference in the magnitude values.

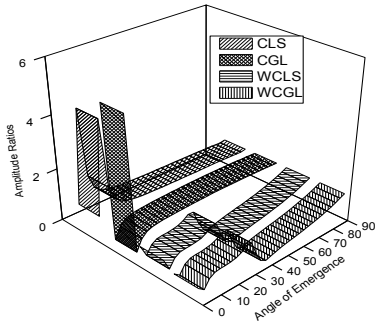

Fig.20
Variation of amplitude ratios of reflected SV1-waves versus angle of incidence.

Fig. 20 represents the variation of amplitude ratio $|Z_3|$ of reflected SV1- wave. It can be observed that the behavior of $|Z_3|$ is reverse for CGL and CLS theories but the behavior is similar for WCLS and WCGL. The values of $|Z_3|$ decrease in $0^o \le \theta_0 \le 4^o$ thereafter it increases as the value of angle of emergence increases for CGL theory. The values of amplitude ratio $|Z_3|$ decrease for small values of θ_0, oscillate for intermediate values and increase for large values of θ_0 for WCLS and WCGL.

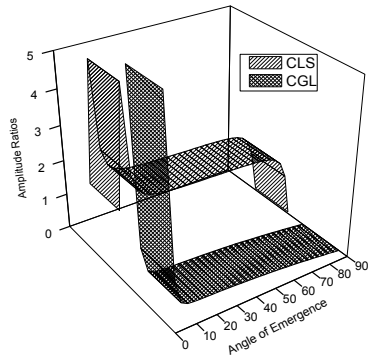

Fig.21
Variation of amplitude ratios of reflected SV2-waves versus angle of incidence.

Fig. 21 depicts the variation of amplitude ratio $|Z_4|$ of reflected SV2- wave. The values of $|Z_4|$ increase when $0^o \le \theta_0 \le 2^o$ and thereafter the values of amplitude ratio $|Z_4|$ decrease with increase in angle of emergence for CLS. The values of amplitude ratio $|Z_4|$ decrease for with the increase in angle of emergence for CGL.

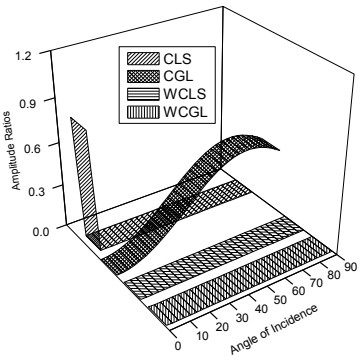

Fig.22
Variation of amplitude ratios of transmitted P-waves versus angle of incidence.

Fig. 22 shows the variation of amplitude ratio $|Z_5|$ for transmitted P-wave. The values of amplitude ratio $|Z_5|$ decrease very sharply for small value of angle of emergence and stationary for the remaining values of angle of emergence for CLS whereas the values of $|Z_5|$ increase for CGL for all values of angle of emergence.

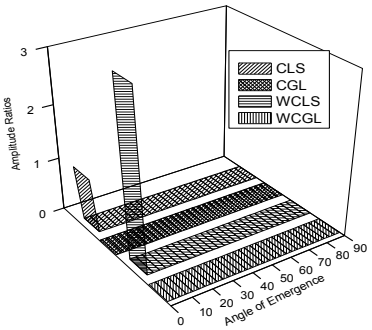

Fig.23
Variation of amplitude ratios of transmitted T-waves versus angle of incidence.

Fig. 23 represents the variation of amplitude ratio $|Z_6|$ of transmitted T-wave. The values of amplitude ratio $|Z_6|$ decrease sharply in the range $0^o \le \theta_0 \le 2^o$ for CLS and WCLS. The values of $|Z_6|$ fluctuate with the increase in the angle of emergence for CGL and WCGL and the values remain very low for the whole range.

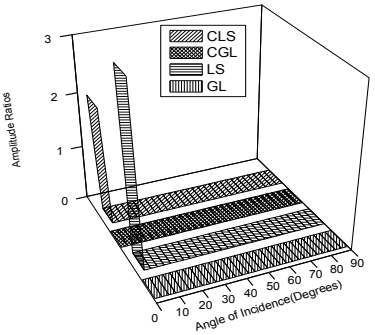

Fig.24
Variation of amplitude ratios of transmitted SV1-waves versus angle of incidence.

Fig. 24 represents the variation of amplitude ratio $|Z_7|$ of transmitted SV1-wave. The values of amplitude ratio $|Z_6|$ decrease sharply in the range $0^o \le \theta_0 \le 2^o$ for CLS. The values of $|Z_7|$ fluctuate with the increase in the angle of emergence for CGL, WCGL and WCLS and the values remain very low for the whole range.

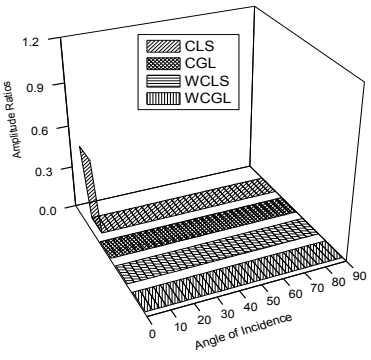

Fig.25
Variation of amplitude ratios of transmitted SV2-waves versus angle of incidence.

Fig. 25 represents the variation of amplitude ratio $|Z_8|$ of transmitted SV2-wave. The values of amplitude ratio $|Z_6|$ decrease sharply in the range $0^o \le \theta_0 \le 2^o$ and decrease smoothly as the value of angle of emergence increases for CLS and WCLS. But the values of $|Z_8|$ remain higher for WCLS in comparison to CLS.

7.4 Incident SV2- wave

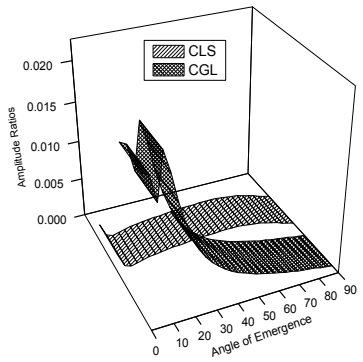

Fig.26
Variation of amplitude ratios of reflected P-waves versus angle of incidence.

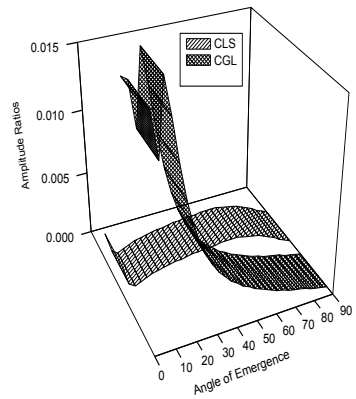

Fig.27
Variation of amplitude ratios of reflected T-waves versus angle of incidence**.**

Fig. 26 shows the variation of amplitude ratio $|Z_1|$ for reflected P-wave. The value of $|Z_1|$ decreases when $0^o \le \theta_0 \le 1.9^o$, increases in the range $1.9^o \le \theta_0 \le 10^o$ and decreases smoothly for the remaining values of θ_0 for CGL. The values of $|Z_1|$ decrease when $0^o \le \theta_0 \le 1.5^o$, increase in $1.5^o \le \theta_0 \le 60^o$ and decrease with the decrease in the values of θ_0 for CLS. Fig. 27 depicts the variation of amplitude ratio $|Z_2|$ for reflected T-wave. The behavior of $|Z_2|$ is similar to that of $|Z_1|$ with change in the magnitude values.

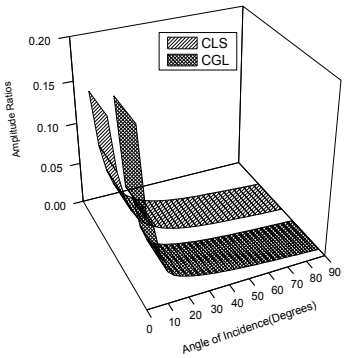

Fig.28
Variation of amplitude ratios of reflected SV1-waves versus angle of incidence.

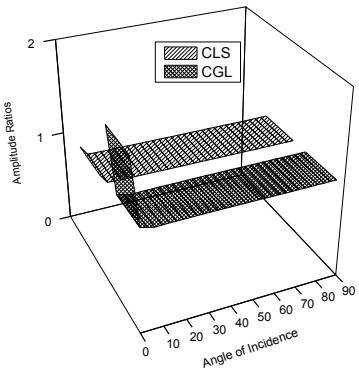

Fig.29
Variation of amplitude ratios of reflected SV2-waves versus angle of incidence.

Figs. 28 and 29 show the variation of amplitude ratio $|Z_3|$ and $|Z_4|$ of reflected SV1- and SV2- waves respectively. It can be observed that the behavior of $|Z_3|$ and $|Z_4|$ is similar with difference in the magnitude values.

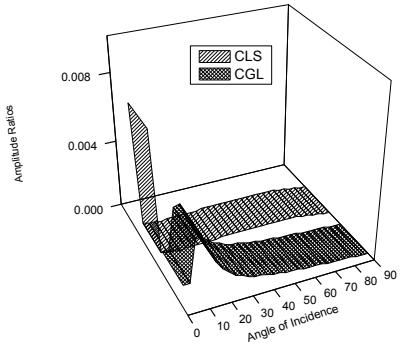

Fig.30
Variation of amplitude ratios of transmitted P-waves versus angle of incidence.

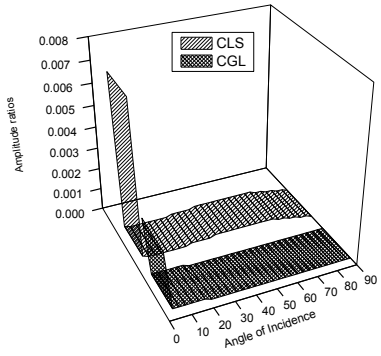

Fig.31
Variation of amplitude ratios of transmitted T-waves versus angle of incidence.

Figs. 30 and 31 depict the variation of amplitude ratio $|Z_5|$ and $|Z_6|$ of transmitted P- and T- waves respectively. It can be observed that the values of $|Z_5|$ and $|Z_6|$ decrease sharply when $0^o \le \theta_0 \le 1^o$ for CLS.

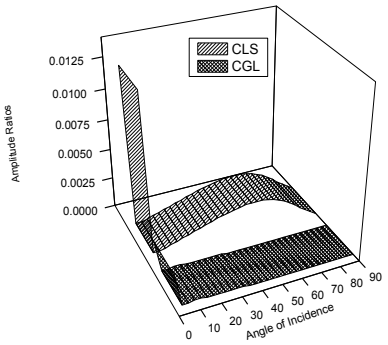

Fig.32
Variation of amplitude ratios of transmitted SV1-waves versus angle of incidence.

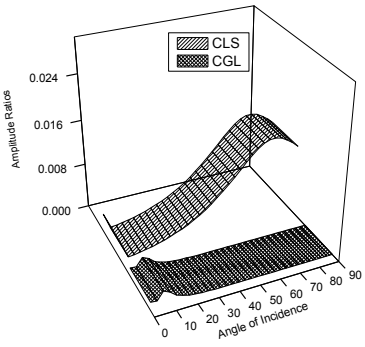

Fig.33
Variation of amplitude ratios of transmitted SV2- waves versus angle of incidence.

Figs. 32 and 33 represent the behavior of amplitude ratio of $|Z_7|$ and $|Z_8|$ of transmitted SV1- and SV2- waves respectively. The values of $|Z_7|$ and $|Z_8|$ decrease sharply for small values of angle of emergence and decrease smoothly for the remaining values of θ_0 for CLS theory whereas the values of amplitude ratios $|Z_7|$ and $|Z_8|$ fluctuate very close to zero for CGL.

8 CONCLUSIONS

The expressions of amplitude ratios of reflection and transmission of waves have been obtained at the interface of two couple stress generalized thermoelastic solids. Some particular cases of interest have been derived from the present investigation. It can be observed that the couple stress effect plays an important role on the reflection and transmission phenomenon. It is observed that the values of amplitude ratio of reflected P-, T- SV1- and SV2- are oscillatory and the values of amplitude ratio of transmitted P-, T- SV1- are decreasing when P- , T- and SV1- wave is incident. The trends of amplitude ratios of reflected P- and T- waves are oscillatory when SV2- wave is incident. The values of reflected SV1-, SV2- and transmitted P-, T-, SV1- and SV2- decrease when SV2- wave is incident. The model studied in the present paper may be helpful to experimental scientists/seismologists working in various fields such as earthquake estimation, and exploration of mineral ores present in the earth's crust.

REFERENCES

[1] Voigt W., 1887, Theoretische studien uber die elastizitatsverhaltnisse der kristalle, *Abhandlungen der Königlichen Gesellschaft der Wissenschaften zu Göttingen* **34**:3-51.

[2] Cosserat E., Cosserat F., 1909, *Theorie des Corps Deformables*, Hermann et Fils, Paris.

[3] Toupin R.A., 1962, Elastic materials with couple-stresses, *Archive for Rational Mechanics and Analysis* **11**(1): 385-414.

[4] Mindlin R.D., Tiersten H.F., 1962, Effects of couple-stresses in linear elasticity, *Archive for Rational Mechanics and Analysis* **11**: 415-448.

[5] Mindlin R.D., 1963, Influence of couple-stresses on stress-concentrations, *Experimental Mechanics* **3**: 1-7.

[6] Koiter W.T., 1964, Couple-stresses in the theory of elasticity, *Proceedings of the Koninklijke Nederlandse Academie van Wetenschappen*, Amsterdam.

[7] Yang J.F.C., Lakes R.S., 1982, Experimental study of micropolar and couple stress elasticity in compact bone in bending, *Journal of Biomechanics* **15**: 91-98.

[8] Yang F., Chong A.C.M., Lam D.C.C., Tong P., 2002, Couple stress based strain gradient theory of elasticity, *International Journal of Solids and Structures* **39**: 2731-2743.

[9] Sengupta P.R., Ghosh B., 1974, Effects of couple stresses on the surface waves in elastic media, *Gerlands Beitr Geophys* **83**:1-18.

[10] Sengupta P.R., Ghosh B., 1974, Effects of couple stresses on the propagation of waves in an elastic layer, *Pure and Applied Geophysics* **112**:331-338.

[11] Sengupta P.R., Benerji D.K., 1978, Effects of couple-stresses on propagation of waves in an elastic layer immersed in an infinite liquid, *International Journal of Pure and Applied Mathematics* **9**:17-28.

[12] Georgiadis H.G., Velgaki E.G., 2003, High-frequency rayleigh waves in materials with micro-structure and couple-stress effects, *International Journal of Solids and Structures* **40**:2501-2520.

[13] Lubarda V.A., Markenscoff X., 2000, Conservation integrals in couple stress elasticity, *Journal of the Mechanics and Physics of Solids* **48**:553-564.

[14] Bardet J.P., Vardoulakis I., 2001, The asymmetry of stress in granular media, *International Journal of Solids and Structures* **38**:353-367.

[15] Lubarda V.A., 2003, Circular inclusions in anti-plane strain couple stress elasticity, *International Journal of Solids and Structures* **40**:3827-3851.

[16] Jasiuk I., Ostoja-Starzewski M., 1995, Planar cosserat elasticity of materials with holes and intrusions, *Applied Mechanics Reviews* **48**(11):S11-S18.

[17] Akgoz B., Civalek O., 2013, Modeling and analysis of micro-sized plates resting on elastic medium using the modified couple stress theory, *Meccanica* **48**(4):863-873.

[18] Sharma V., Kumar S., 2014, Velocity dispersion in an elastic plate with microstructure: effects of characteristic length in a couple stress model, *Meccanica* **49**:1083-1090.

[19] Biot M., 1956, Thermoelasticity and irreversible thermodynamics, *Journal of Applied Physics* **27**: 240-253.

[20] Lord H., Shulman Y., 1967, A generalized dynamical theory of elasticity, *Journal of the Mechanics and Physics* **15**: 299-309.

[21] Green A.E., Lindsay K.A., 1972, Thermoelasticity, *Journal of Elasticity* **2**: 1-7.

[22] Ram P., Sharma N., 2008, Reflection and transmission of micropolar thermoelastic waves with an imperfect bonding, *International Journal of Applied Mathematics and Mechanics* **4**(3): 1-23.

[23] Xue B.B., Xu H.Y., Fu Z.M., Sun Q.Y., 2010, Reflection and refraction of longitudinal displacement wave at interface between two micropolar elastic solid, *Advanced Materials Research* **139-141**: 214-217.

[24] Kumar R., Kaur M., Rajvanshi S.C., 2014, Reflection and transmission between two micropolar thermoelastic half-spaces with three-phase-lag model, *Journal of Engineering Physics and Thermophysics* **87**(2): 295-307.